Electronic Supplementary Material (ESI) for ChemComm.

Water oxidation using copper(2-(2′-pyridyl)imidazole): catalytic enhancement from an ionisable imidazole ligand

Leea A. Stott, Kathleen E. Prosser, Ellan K. Berdichevsky,
Charles J. Walsby and Jeffrey J. Warren*

Department of Chemistry
Simon Fraser University
8888 University Drive
Burnaby BC V5A1S6
Canada

Email: j.warren@sfu.ca

Contents:

1. Materials and methods

All reagents were purchased from Sigma-Aldrich unless otherwise noted and used without further purification. Copper(II) acetate was from Mallinckrodt . Gases were obtained from Praxair Canada. ^{1}H NMR were recorded on a Bruker Ultrashield Plus 400 or 500 MHz instruments Solvent residual signals used as references.[1] UV-visible spectra were recorded using a Cary100 UV-Vis spectrophotometer at ambient temperature. EPR measurements were performed at X-band (9.3−9.4 GHz) using a Bruker EMXplus spectrometer with a PremiumX microwave bridge and HS resonator. In all cases, sample temperature was 100 K.

Basal plane graphite electrodes were prepared according to the literature.[2] Pyrolytic graphite was from www.graphitestore.com, Loctite Hysol 9460 epoxy was obtained from McMaster-Carr, and sliver paint was from SPI Supplies. ITO glass was from www.adafruit.com. Electrochemical contacts were made with a small amount of silver paint, which was then covered with epoxy. Electrodes were sonicated briefly in isopropyl alcohol prior to experiments.

All electrochemical measurements were performed on a CH Instruments 6171B potentiostat, using a conventional three-electrode cell with a basal plane graphite working electrode (3 mm by 3 mm surface area), Pt wire counter electrode, and aqueous Ag/AgCl (saturated KCl) reference electrode (CH Instruments). The working electrode surfaces were prepared by lightly abrading 0.3 μm alumina power with a microcloth polishing pad (Buehler), washing thoroughly with deionised water, and briefly drying with a heat gun. Potassium ferricyanide ($E°$ = 0.436 V versus NHE) was used as an external standard for all electrochemical experiments and all potentials are reported with respect to the normal hydrogen electrode (NHE). Oxygen was detected using a Vernier Optical Dissolved Oxygen Probe.

1. Fulmer, G. R., Miller, A. J. M., Sherden, N. H., Gottlieb, H. E., Nudelman, A., Stoltz, B. M., Bercaw, J. E., and Goldberg, K. I. *Organometallics* **2010**, *29*, 2176-2179.
2. Blakemore, J. D., Schley, N. D., Balcells, D., Hull, J. F., Olack, G. W., Incarvito, C. D., Eisenstein, O., Brudvig, G. W., and Crabtree, R. H. *J. Am. Chem. Soc.* **2010**, *132*, 16017-16029.

2. Synthesis.

pimH[3] An ice-cold solution of 2-pyridinecarboxyaldehyde (4.668 mmol) in 5 mL ethanol was added to an ice-cold solution of 40% aqueous glyoxal (0.2 mL) in 5 mL ethanol, and then ice-cold concentrated aqueous NH_4OH solution (0.15 mL) was added immediately. This solution was stirred at 0°C for 1 h, warmed to room temperature, and stirred for an additional 5 h. The solvent was removed under reduced pressure, and the resulting solution was extracted several times with diethyl ether. The combined organic extracts were evaporated under reduced pressure and crystalline solids were obtained upon recrystallization with diethyl ether.

PyIm. Pale yellow solid. Yield: 41%. ^{1}H NMR (400MHz, $CDCl_3$): δ (ppm) 11.7 (s, 1H) 8.51 (ddd, 1H, 4.9, 1.8, 1.0 Hz), 8.24 (dt, 1H, 8.0, 1.1 Hz), 7.80 (td, 1H, 7.8 1.7 Hz), 7.26 (ddd, 1H, 7.6, 4.9, 1.2 Hz), 7.17 (br s, 2H).

3. Wang, R., Xiao, J.-C., Twamley, B., and Shreeve, J. M. *Org. Biomol. Chem.* **2007**, *5*, 671-678.

3. Cyclic voltammetry experiments

Equimolar amounts of $Cu(OAc)_2$ and 2-(2´-pyridyl)imidazole) were mixed in 0.1 M aqueous sodium acetate to give a pale blue solution. The pH was adjusted using 5M NaOH solution. Cyclic voltammograms (CVs) were obtained for different pH values and catalyst concentrations. CVs were recorded under air using the setup described above. All potentials are reported versus the normal hydrogen electrode (NHE) by adjustment based on calibration against potassium ferricyanide ($E°´_7$ = 0.436 V).

4. Concentration dependence of CVs

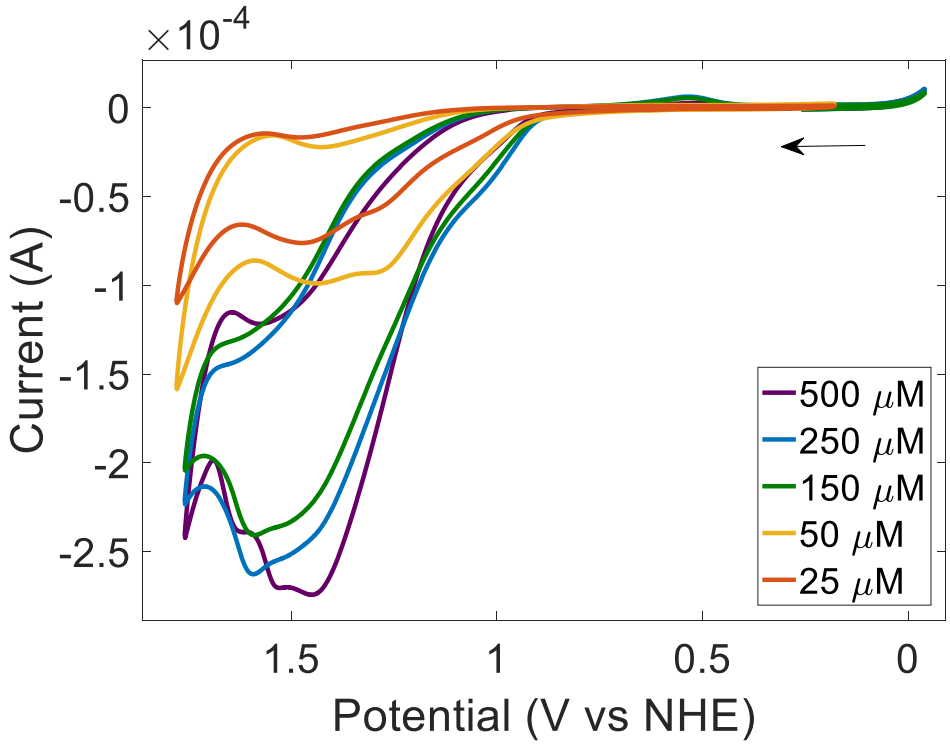

Figure S1. Concentration dependence of 1:1 mixtures of Cu^{2+} and pimH (150 μM each) at pH 12.1. Scan rate = 100 mV s^{-1}.

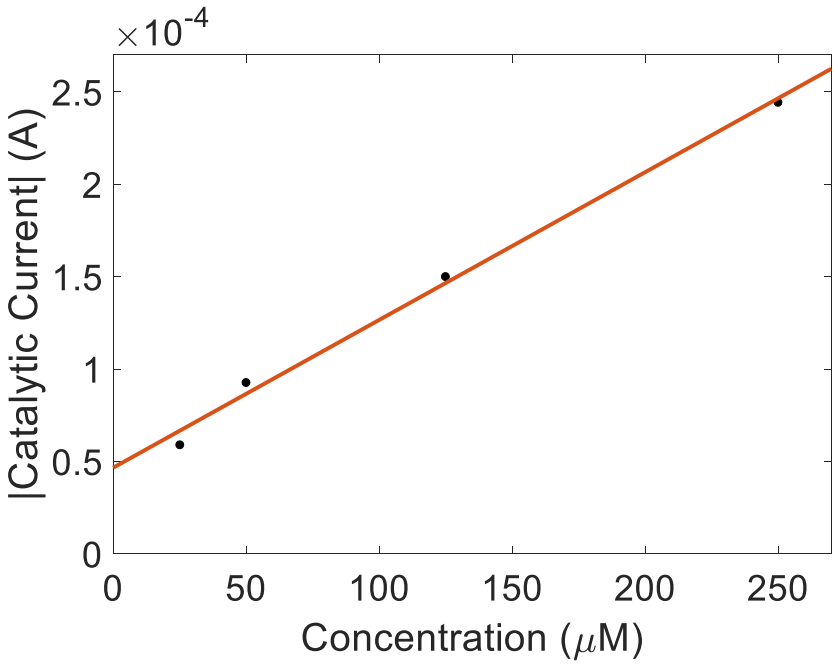

Figure S2. Plot of absolute current at ~1.3V as a function of concentration. The current taken at the second inflection point (~1.3V) of each CV yielded.

5. Scan rate dependence

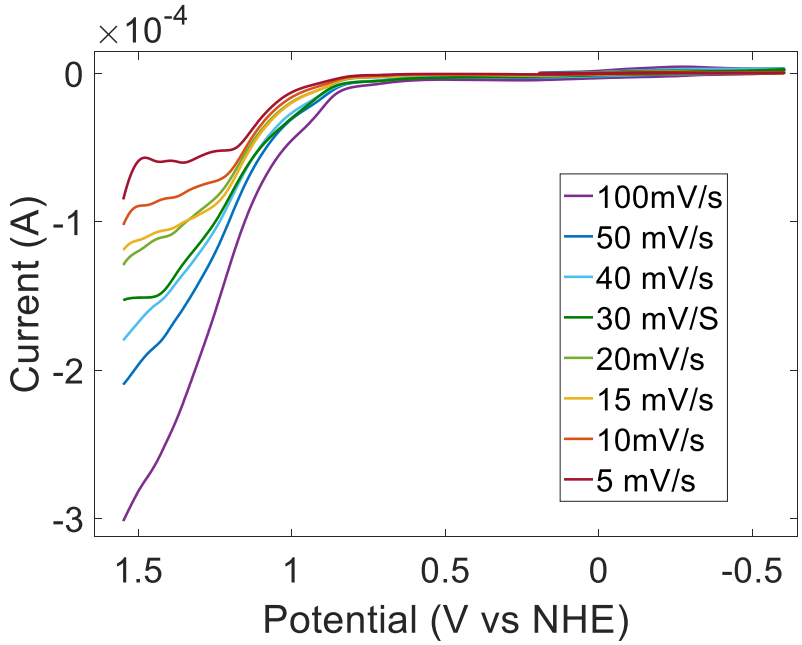

Figure S3. Scan rate dependence of 50 μM $Cu(OAc)_2$ + 50 μM pimH in 0.1 M NaOAc, pH 12.24.

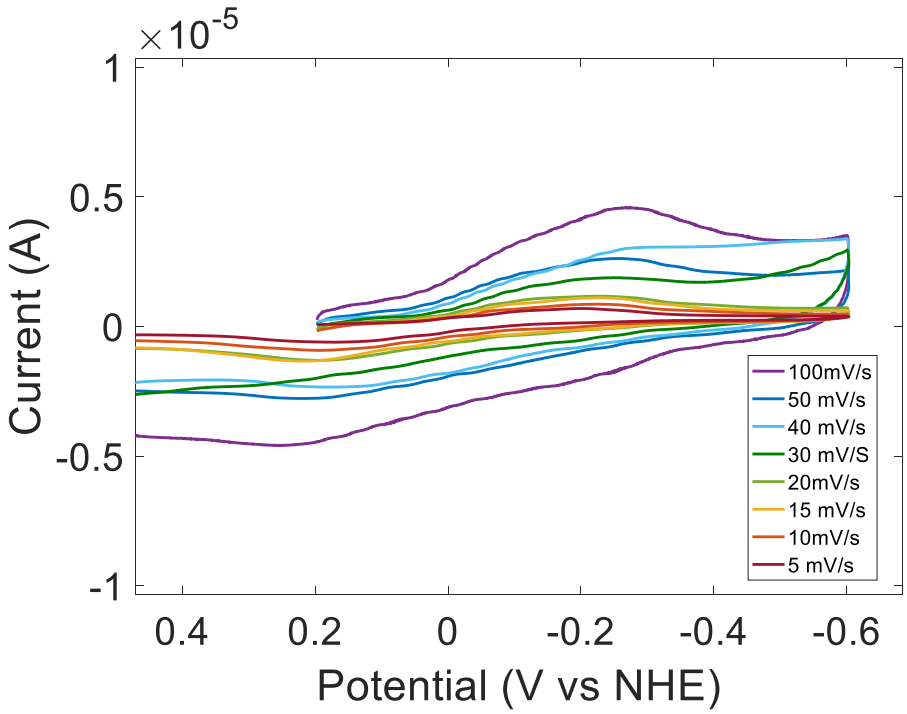

Figure S4. Scan rate dependence on the quasireversible $Cu^{2+/+}$ couple in 50 μM $Cu(OAc)_2$ + 50 μM pimH in 0.1 M NaOAc, pH 12.24.

6. Turnover frequency analysis

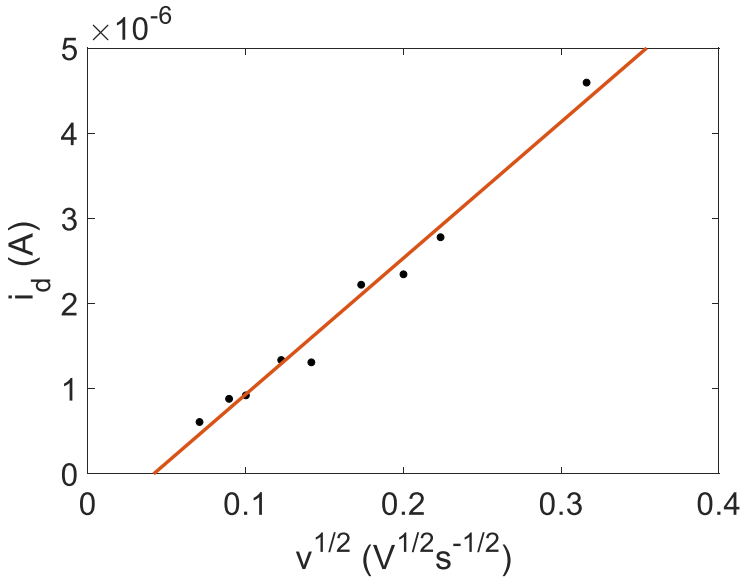

Figure S5. Plot of square root of scan rate versus diffusive current at ~0.2 V from Figure S4.

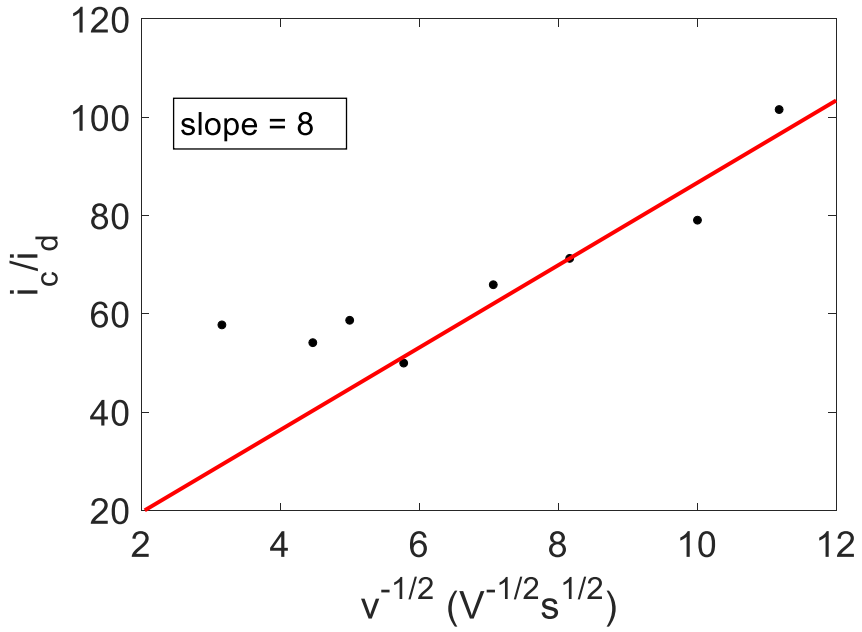

Figure S6. Plot of the inverse of the square root of scan rate versus the ratio of catalytic current to diffusive current according to the ratio of Eqn 1 (main text and the Randles-Sevcik equation: $i_d=0.4463n_dFA[Cu](n_dFvD_{Cu}/RT)^{1/2}$ where n_d is the electrons transferred in the non-catalytic reaction, R is the gas constant, T is the absolute temperature and v is the scan rate.

7. Background current response (electrode, pimH) and homogeneous catalysis test

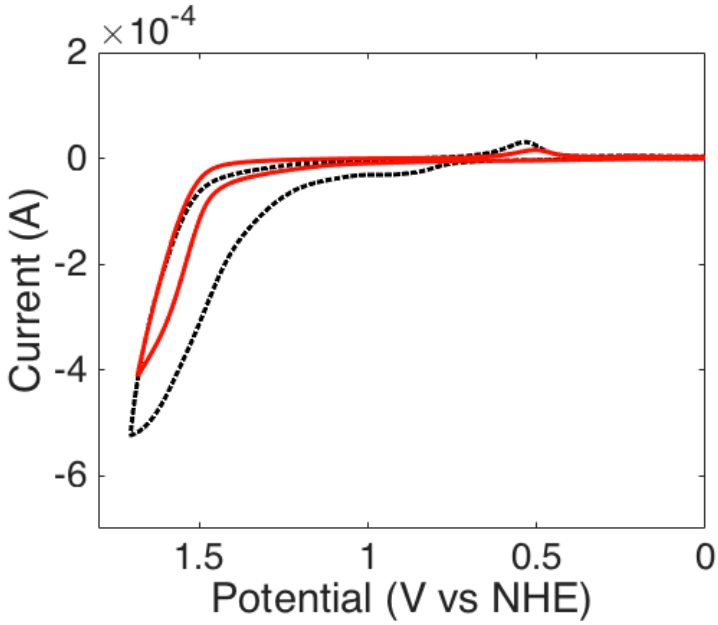

Figure S7. Comparison of background current 0.1 NaOAc, pH 12.1 at a bare BPG electrode (red solid pline) or 150 μM pimH in 0.1 M NaOAc, pH 12.1 (black dashed line).

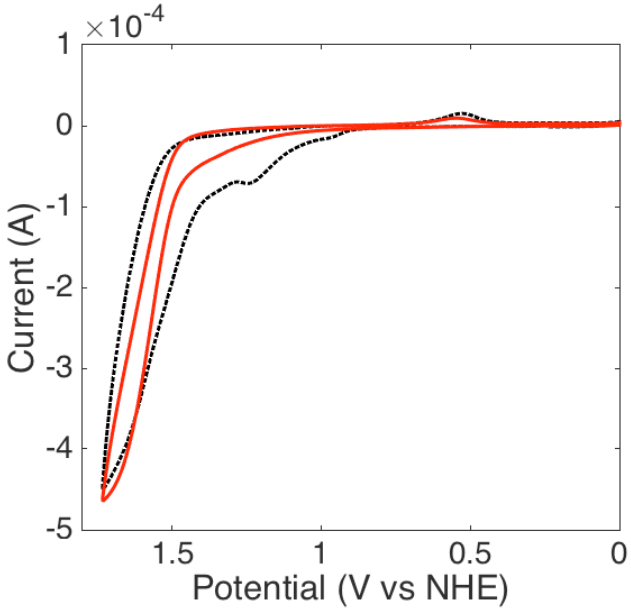

Figure S8. A polished electrode was used for CVs of 150 μM $Cu(OAc)_2$ + 150 μM pimH) (0.1 M NaOAc, pH 12.2) for several cycles. The electrode was then removed from the solution, rinsed with DI water and then CVs were collected in fresh 0.1 M NaOAc, pH 12.2.

8. Controlled potential electrolysis

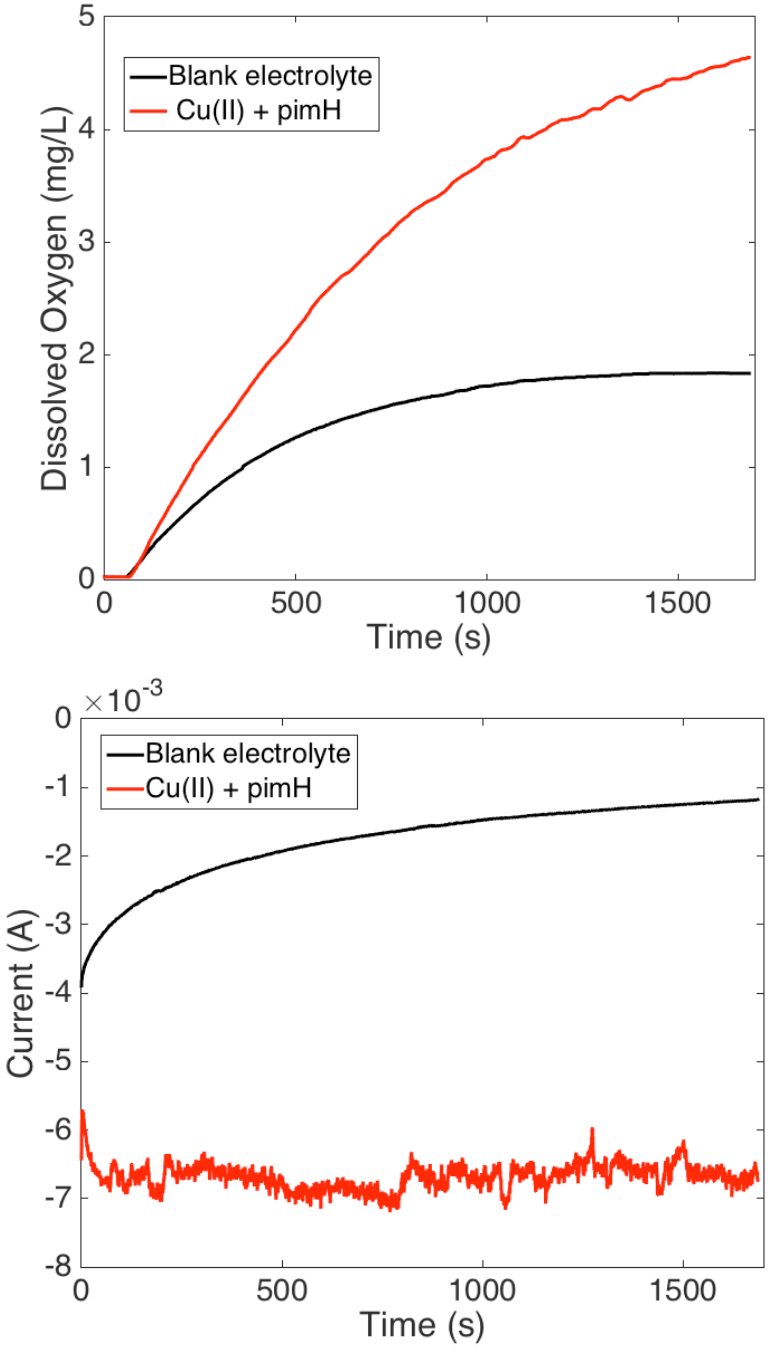

Figure S9. Top: Dissolved O_2 detected as a function of time in controlled potential electrolysis experiments (1.1 V versus NHE applied potential) using 250 μM $Cu(OAc)_2$ + pimH in 0.1 M NaOAc electrolyte, pH 12.1 and a 3.4 cm^2 ITO electrode. Bottom: current as a function of time for the same experiment. In both plots, the red trace corresponds to Cu/pimH solution and the black trace to NaOAc alone.

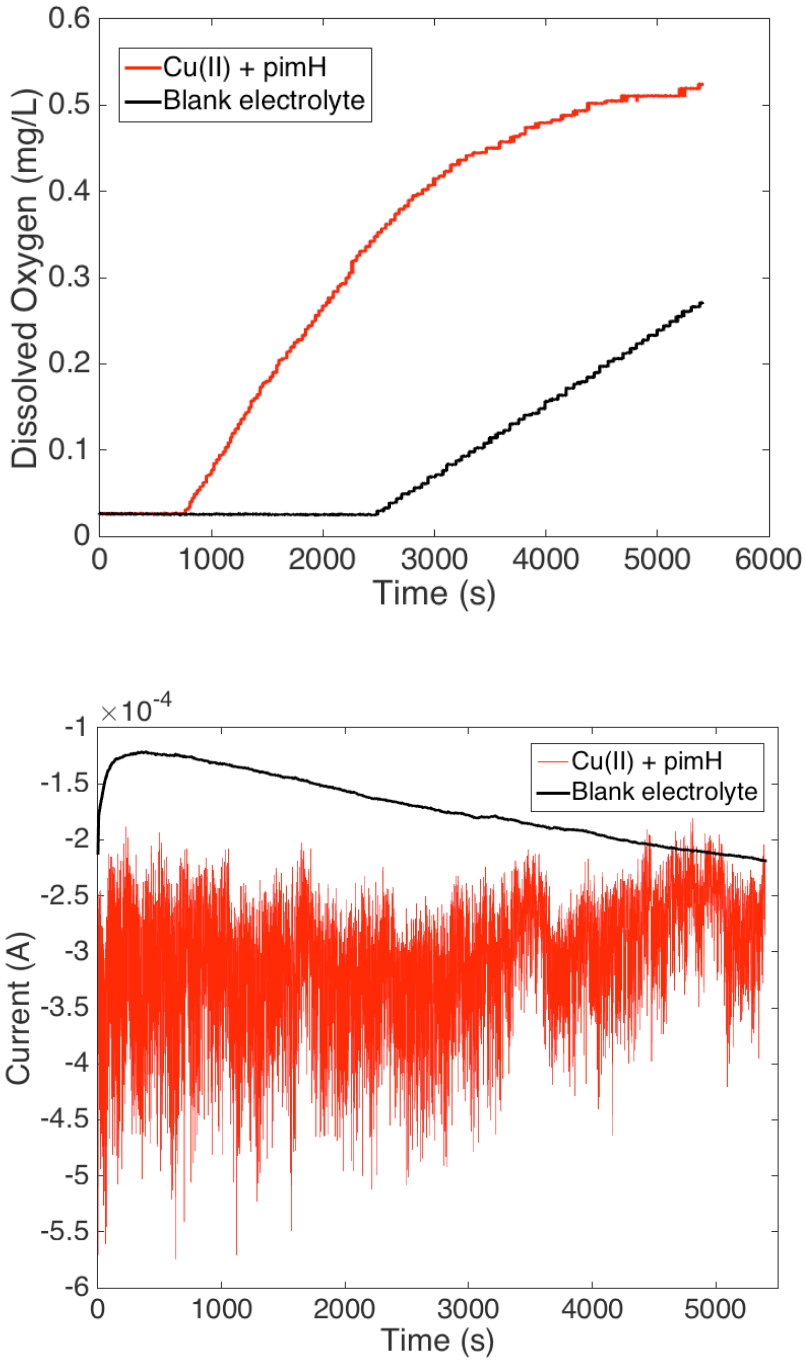

Figure S10. Top: Dissolved O_2 detected as a function of time in controlled potential electrolysis experiments (1.1 V versus NHE applied potential) using 250 μM $Cu(OAc)_2$ + pimH in 0.1 M NaOAc electrolyte, pH 12.1 and a 0.09 cm^2 basal plane graphite electrode. Bottom: current as a function of time for the same experiment. In both plots, the red trace corresponds to Cu/pimH solution and the black trace to NaOAc alone.

9. Optical spectra Cu^{II} + pimH (pH 4-13)

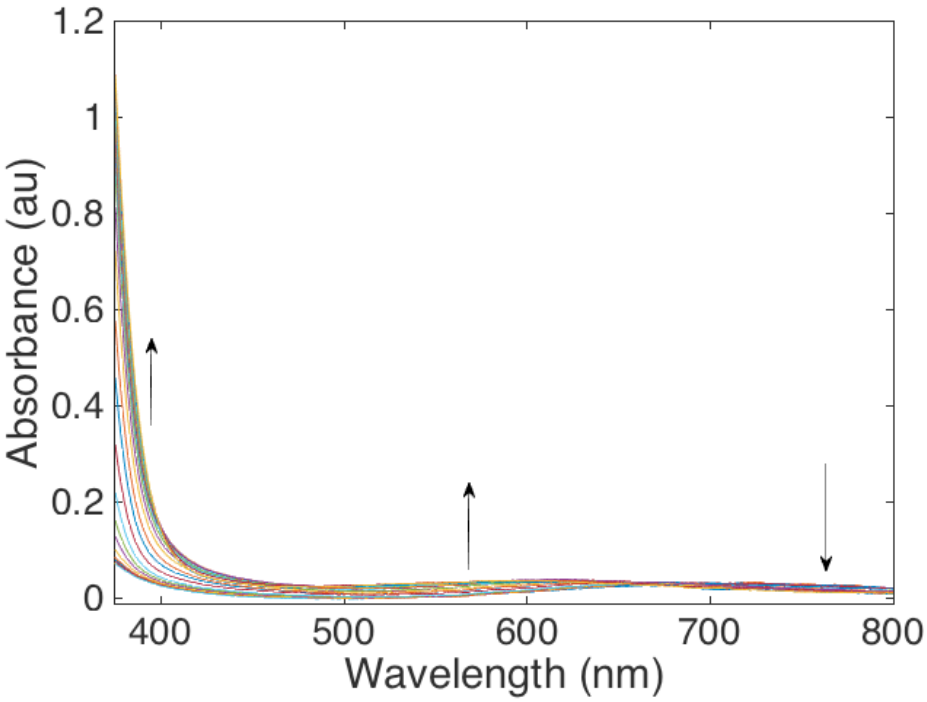

Figure S11. Optical spectra of 150 μM $Cu(OAc)_2$ + 150 μM pimH between pH 4.0 and 13.7. The arrows indicate the progressive changes in absorbance as a function of increasing pH.

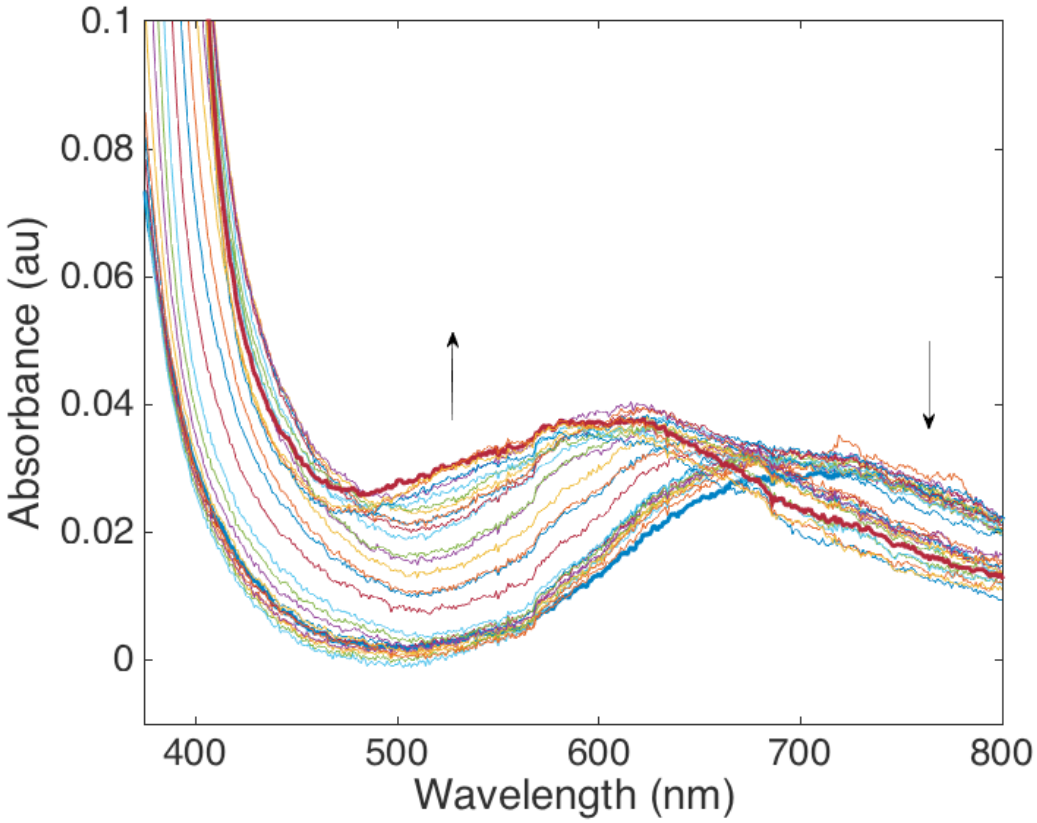

Figure S12. Magnified low energy region of Figure S8. Optical spectra of 150 μM $Cu(OAc)_2$ + 150 μM pimH between pH 4.0 and 13.7. The arrows indicate the progressive changes in absorbance as a function of increasing pH. The bold spectra represent starting and ending pH values.

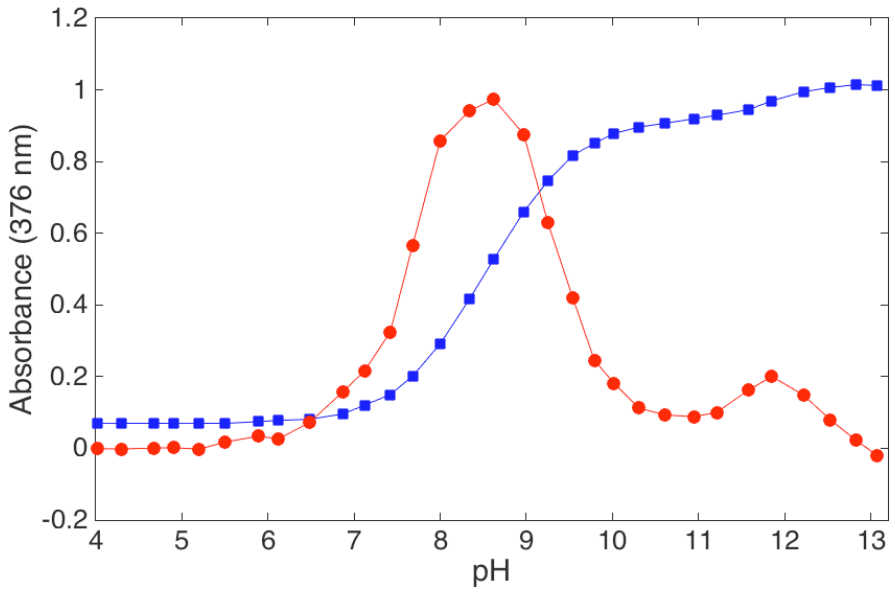

Figure S13. Plot of absorbance at 376 nm (from Figure S8) as a function of pH (blue squares). The red circles are the numerical derivative of the data shown in blue to show the inflection points.

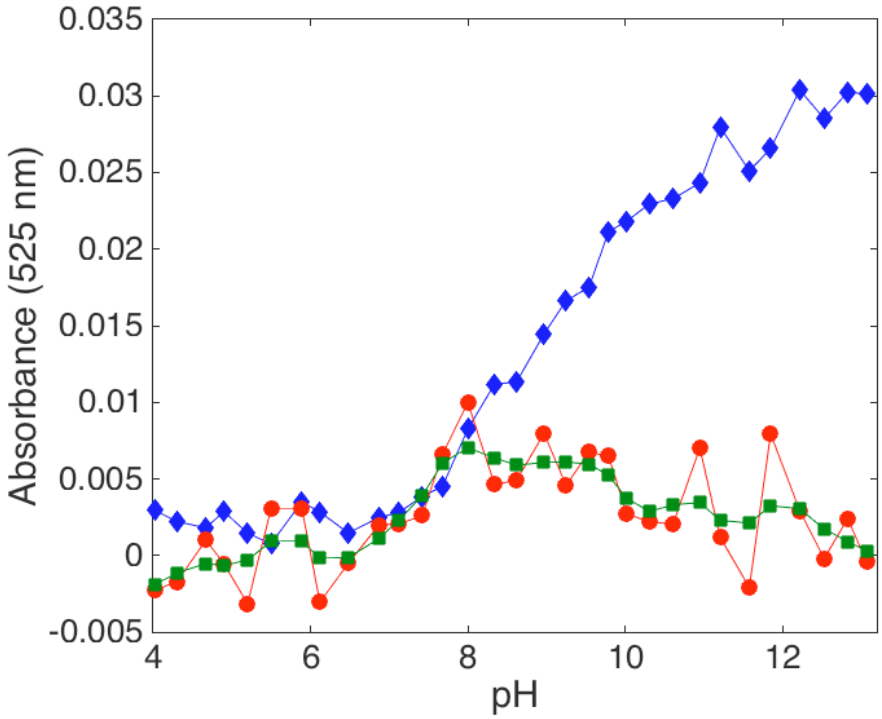

Figure S14. Plot of absorbance 525 nm (from Figure S8) as a function of pH (blue diamonds). The red circles are the numerical derivative of the data shown in blue to show the inflection points. The green squares are a smoothed (moving average) numerical derivative of the data shown in blue.

10. EPR spectra and simulations (pH 8-12)

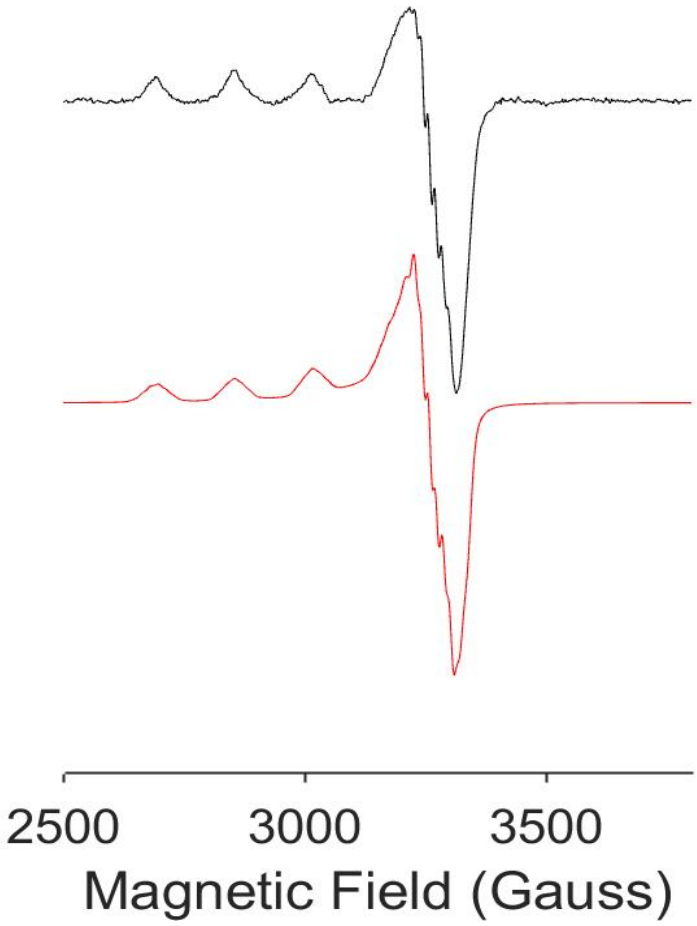

Figure S15. EPR Spectrum of 150 μM $Cu(OAc)_2$ + 150 μM pimH, pH 8. The experimental data are shown in black and a simulation of the weighted sum of EPR active species is shown in red. Simulation variables can be found in Table 1.

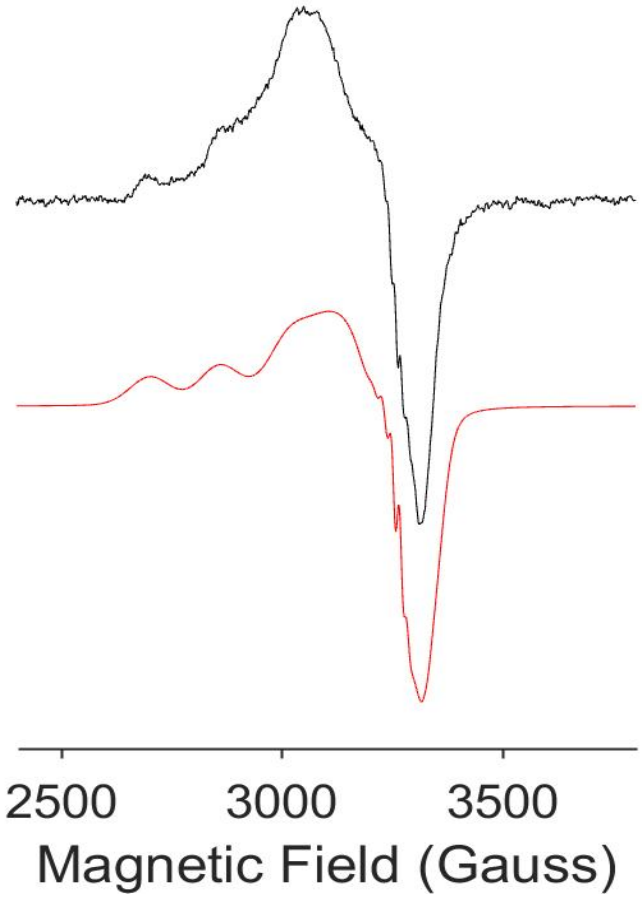

Figure S16. EPR Spectrum of 150 μM $Cu(OAc)_2$ + 150 μM pimH, pH 9. The experimental data are shown in black and a simulation of the weighted sum of EPR active species is shown in red. Simulation variables can be found in Table 1.

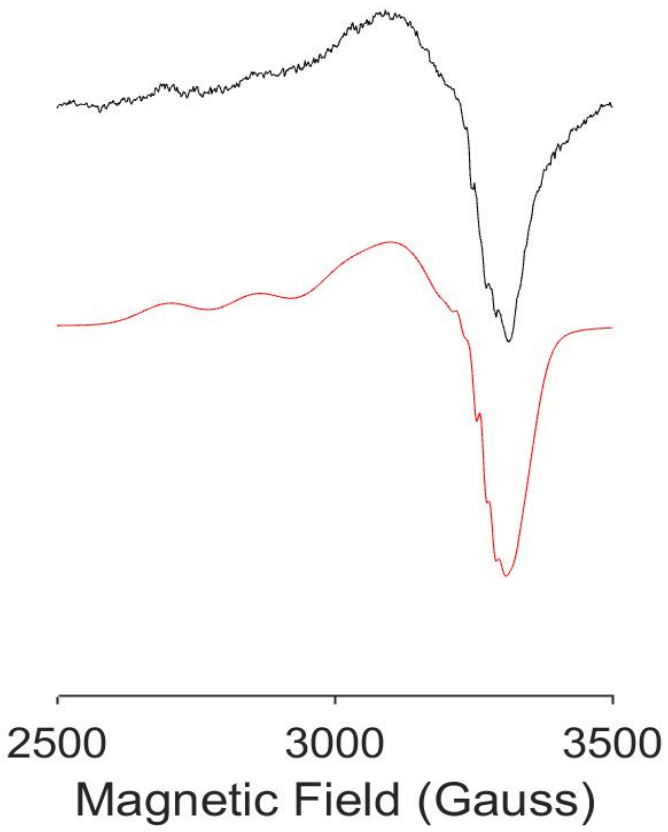

Figure S17. EPR Spectrum of 150 μM $Cu(OAc)_2$ + 150 μM pimH, pH 10. The experimental data are shown in black and a simulation of the weighted sum of EPR active species is shown in red. Simulation variables can be found in Table 1.

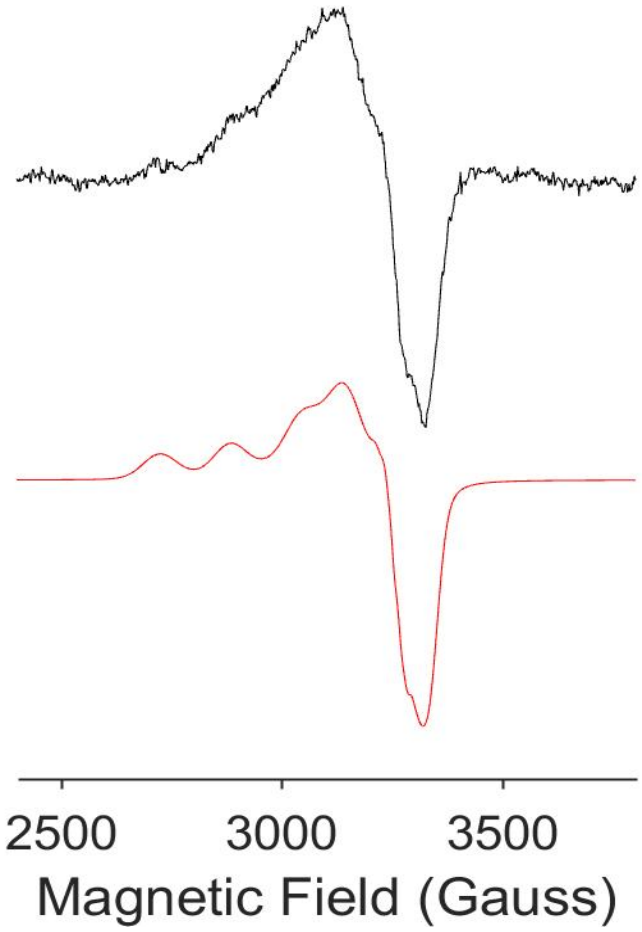

Figure S18. EPR Spectrum of 150 μM $Cu(OAc)_2$ + 150 μM pimH, pH 11. The experimental data are shown in black and a simulation of the weighted sum of EPR active species is shown in red. Simulation variables can be found in Table 1.

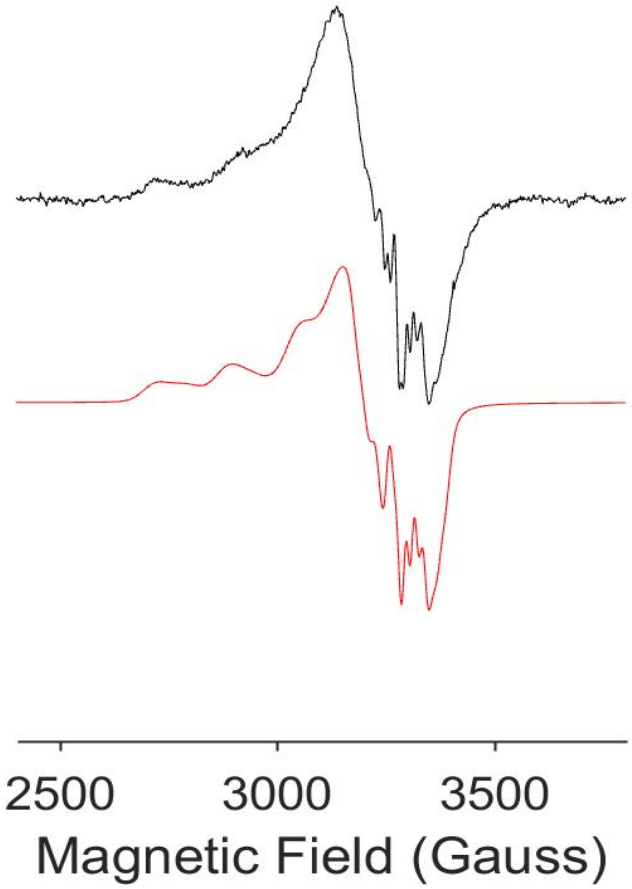

Figure S19. EPR Spectrum of 150 μM $Cu(OAc)_2$ + 150 μM pimH, pH 12. The experimental data are shown in black and a simulation of the weighted sum of EPR active species is shown in red. Simulation variables can be found in Table 1.

11. Summary of EPR simulation parameters

Table 1. EPR parameters for each species at corresponding pH. Certain hyperfine values are not reported due to the unresolved features arising from other solution components. [a]

pH	Species	$g_{\perp}$	$g_{\|\|}$	$A_{\perp}$	$A_{\|\|}$	$A_{\perp}$	$A_{\|\|}$
8	a	2.059	2.285	10	181	14	18
9	a	2.051	2.285	11.5	182	22	23
	b	2.12	2.285	-	-	-	-
10	a	2.054	2.285	11.5	182	22	23
	b	2.12	2.285	-	-	-	-
11	a	2.054	2.265	11	180	14.5	15
	b	2.11	2.265	-	-	-	-
12	a	2.034	2.264	15	182	19	17
	b	2.078	2.268	-	-	-	-
	c	2.105	2.24	-	-	-	-

[a] Values shown for ^{63}Cu. All simulations include contributions from ^{63}Cu and ^{65}Cu according to natural abundance.